

Selective lithium halide ion-pair sensing by a dynamic metalloporphyrin [2]rotaxane

Jamie T. Wilmore^a, Andrew Docker^b, Paul D. Beer^{*a}

^a Chemistry Research Laboratory, Department of Chemistry, University of Oxford, Mansfield Road, Oxford, UK, OX1 3TA

^b Yusuf Hamied Department of Chemistry, University of Cambridge, Lensfield Road, Cambridge, CB2 1EW

* paul.beer@chem.ox.ac.uk

Supporting Information

Table of Contents

S1 General Experimental Procedures	S2
S2 Novel Compound Synthesis	S3
S3 Spectral Characterisation of Novel Structures	S6
S4 Investigation of Macrocyclic Shuttling Barrier	S10
S5 Measurement of the 'Resting State' Bias	S11
S6 ¹ H NMR Binding Studies	S12
S7 Optical Titration Studies of TBAX Salt Anion Binding.....	S14
S8 References.....	S16

S1 General Experimental Procedures

Solvents and reagents were purchased from commercial suppliers and used as received. Dry solvents were obtained by purging with nitrogen and passing through a MBraun MPSP-800 column. H₂O was de-ionised and micro-filtered using a Milli-Q® Millipore machine.

Experiments were conducted at room temperature unless otherwise stated. Merck silica gel 60 was used for flash column chromatography. Inorganic salts used in binding studies were purchased from commercial suppliers and stored in vacuum desiccators prior to use.

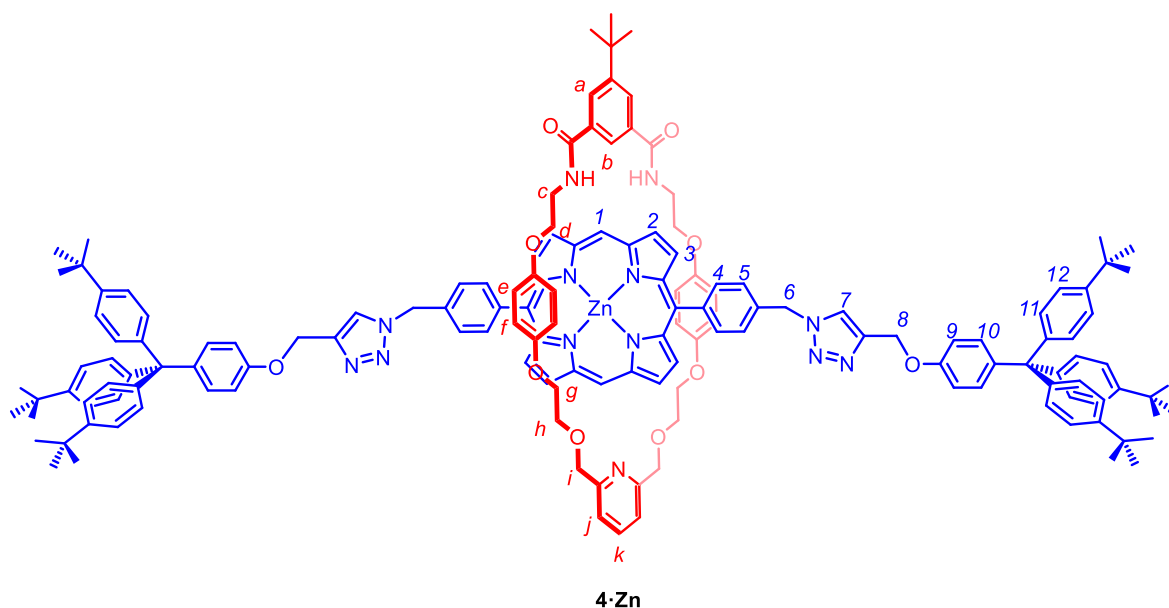
NMR spectra were either recorded on a Bruker Avance III HD Nanobay NMR spectrometer equipped with a 9.4 T magnet or a Bruker NEO 600 with broadband helium cryoprobe. ¹H NMR titrations were recorded on a Bruker Avance III NMR equipped with a 11.75 T magnet. Chemical shifts are quoted in parts per million relative to the residual solvent peak.

UV-visible absorption spectra were measured at 298 K using a Horiba Duetta, using quartz cuvettes with a path length of 10 mm.

The following compounds were prepared according to literature procedures: **1**,¹ **2·Zn²** and **3**.³

S2 Novel Compound Synthesis

Heteroditopic Zn(II)-Metalloporphyrin [2]Rotaxane **4·Zn**



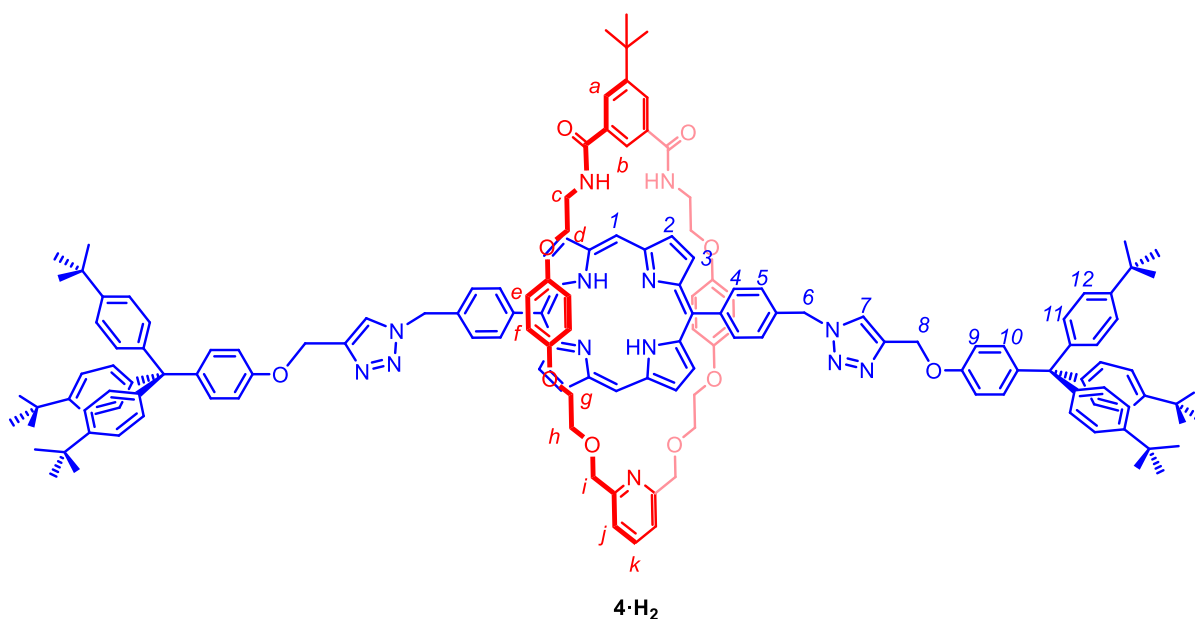
Macrocycle **1** (14.2 mg, 0.021 mmol)¹ and [Cu(MeCN)₄]PF₆ (7.7 mg, 0.021 mmol) were added to degassed dry DCE (1.6 mL) in a sealed flask. The mixture was purged with N₂ for 10 min, and stirred at room temperature for 30 min. Stopper alkyne **3** (68.0 mg, 0.125 mmol)⁴ and the *para*-metalloporphyrin bis-azide **2·Zn** (39.1 mg, 0.061 mmol) were dissolved in degassed dry DCE (3 mL) and the resulting solution purged with N₂ for 5 min. The porphyrin solution was added dropwise to the copper solution, and the reaction mixture heated to 60 °C for 3 days. The reaction was cooled to room temperature and the solvent removed *in vacuo*. The residue was taken up in DCM (30 mL) and washed with aqueous NH₄OH/EDTA (2 x 20 mL) and water (20 mL). The combined aqueous layers were re-extracted with further DCM (20 mL) and the combined organic layers dried over MgSO₄ and the volatiles removed *in vacuo*. **4·Zn** was obtained by preparative TLC (4% MeOH *v/v* in DCM, followed by 2:89:9 *v/v* MeOH:DCM:EtOAc) as a red solid. Yield: 36.9 mg (73%).

¹H NMR (500 MHz, CDCl₃, 338 K) δ : 10.22 (s, 2H, *H*₁), 9.37 (d, *J* = 4.4 Hz, 2H, *H*₂), 8.94 (broad s, 2H, *H*₃), 8.14 (d, *J* = 7.4 Hz, 4H, *H*₄), 7.85 (app s., 1H, *H*_k), 7.65 (m, 4H, *H*_{a,j}), 7.56-7.41 (m, 11H, *H*_{5,7,10 b}), 7.29 (d, *J* = 8.7 Hz, 12H, *H*₁₁), 7.15 (d, *J* = 8.7 Hz, 12H, *H*₁₂), 6.82 (d, *J* = 8.5 Hz, 4H, *H*₉), 6.71 (d, *J* = 8.8 Hz, *H*_e), 6.64 (d, *J* = 8.8 Hz, *H*_f), 5.68 (s, 4H *H*₆), 5.44 – 5.36 (m, 2H, *H*_{NH}), 4.94 (s, 4H, *H*₈), 4.64 (s, 4H, *H*_i), 4.10 (s, 4H, *H*_d), 3.90-3.84 (m, 8H, *H*_{g,h}), 3.42 (s, 4H, *H*_c), 1.34 (s, 54H, *H*_{stopper tBu}), 1.32 (s, 9H, *H*_{tBu}) ppm.

$^{13}\text{C}\{^1\text{H}\}$ NMR (151 MHz, CDCl_3) δ : 167.9, 157.4, 155.8, 153.1, 152.4, 152.0, 149.7, 149.5, 148.4, 144.0, 143.6, 143.4, 140.4, 134.8, 133.6, 133.2, 132.4, 132.0, 131.8, 130.7, 127.9, 125.6, 124.1, 121.0, 118.5, 115.8, 115.5, 113.1, 106.2, 74.3, 69.9, 68.3, 66.5, 63.1, 39.3, 34.8, 34.3, 33.2, 31.9, 31.4 31.0, 29.7, 29.4 ppm. Undetected aromatic signals believed to be coincident.

HR-ESI-MS m/z calculated for $[\text{C}_{153}\text{H}_{160}\text{O}_{10}\text{N}_{13}\text{Zn}]^+$, $[\text{M}+\text{H}]^+$: 2403.1697, found: 2403.1708.

Heteroditopic Free-base Porphyrin [2]Rotaxane **4**·**H**₂



Trifluoroacetic acid (0.05 mL, 0.66 mmol) was added dropwise to a solution of **4**·**Zn** (16 mg, 6.60 μmol) in dry DCM (5 mL) in a sealed flask before stirring for four hours at room temperature. Aqueous NaHCO_3 (1.0 M) was added to the reaction mixture until effervescence ceased, whereupon an additional 10 mL was added. The organic layer was collected and the aqueous layer further extracted with DCM (10 mL x 3). The combined organic layers were washed with 1.0 M NaHCO_3 (20 mL) and H_2O (30 mL x 4) and dried over MgSO_4 . The solvent was removed *in vacuo* affording **4**·**H**₂ as a red solid. Yield: 14.3 mg (92%).

^1H NMR (600 MHz, CDCl_3) δ : 10.32 (s, 2H, H_1), 9.39 (d, $J = 4.5$ Hz, 4H, H_2), 8.98 (d, $J = 4.5$ Hz, 4H, H_3), 8.31 (s, 1H, H_b), 8.21 (m, 6H, $H_{4,7}$), 7.64 (s, 2H, H_a), 7.58 (m, 6H, $H_{5,j}$), 7.33 (t, $J = 7.6$ Hz, 1H, H_k), 7.25 – 7.22 (d, $J = 8.5$ Hz, 12H, H_{11}), 7.15 (d, $J = 8.3$ Hz, 4H, H_{10}), 7.10 (d, $J = 8.5$ Hz, 12H, H_{12}), 6.81 (d, $J = 8.3$ Hz, 4H, H_9), 6.64 (d, $J = 8.7$ Hz, 4H $H_{e \text{ or } f}$), 6.48 (d, $J = 8.7$ Hz, 4H $H_{e \text{ or } f}$), 5.65 (s, 4H, H_6), 5.04 (s, 4H, H_8), 4.65 (s, 4H, H_i), 4.04 – 3.99 (m, 4H, H_d), 3.89 – 3.84 (m, 8H, $H_{g,h}$), 3.77 (m, 4H, H_c), 1.30 (s, 54H, $H_{\text{stopper tBu}}$), 1.26 (s, 9H, $H_{\text{macrocycle tBu}}$), -3.15 (s, 2H, H_{NH}) ppm.

$^{13}\text{C}\{^1\text{H}\}$ NMR (151 MHz, CDCl_3) δ : 167.8, 157.7, 156.0, 153.0, 152.6, 152.5, 148.4, 146.9, 145.3, 144.7, 144.1, 142.0, 140.5, 137.1, 135.4, 134.1, 133.9, 132.4, 132.0, 130.9, 130.7, 128.8, 126.8, 123.4, 121.5, 118.0, 115.7, 115.4, 113.2, 105.6, 74.1, 69.7, 68.2, 66.9, 63.1, 61.7, 54.1, 53.4, 39.9, 35.0, 34.3, 31.2, 30.9, 29.7 ppm.

HR-ESI-MS m/z calculated for $[\text{C}_{153}\text{H}_{162}\text{O}_{10}\text{N}_{13}]^+$, $[\text{M}+\text{H}]^+$: 2341.2562, found: 2341.2523.

S3 Spectral Characterisation of Novel Structures

4·Zn

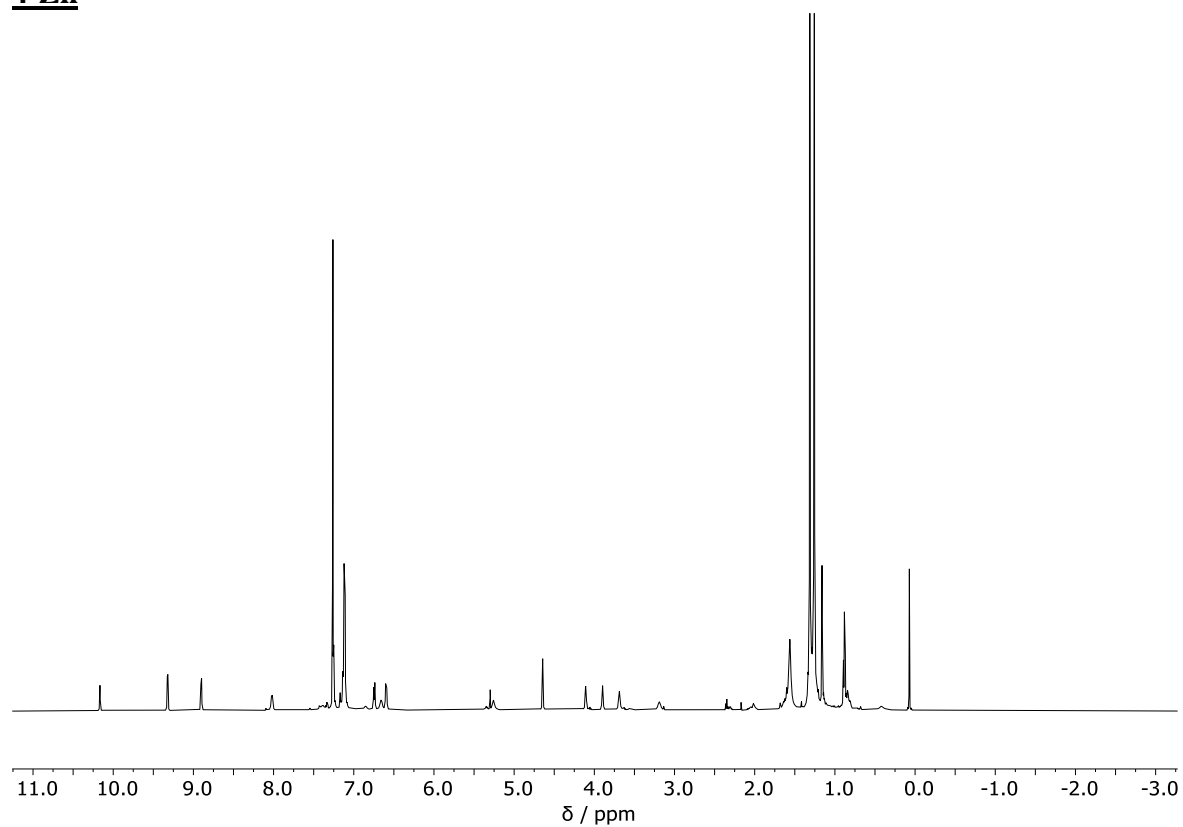


Figure S1. ^1H NMR spectrum (600 MHz, CDCl_3 , 298 K) of **4·Zn**.

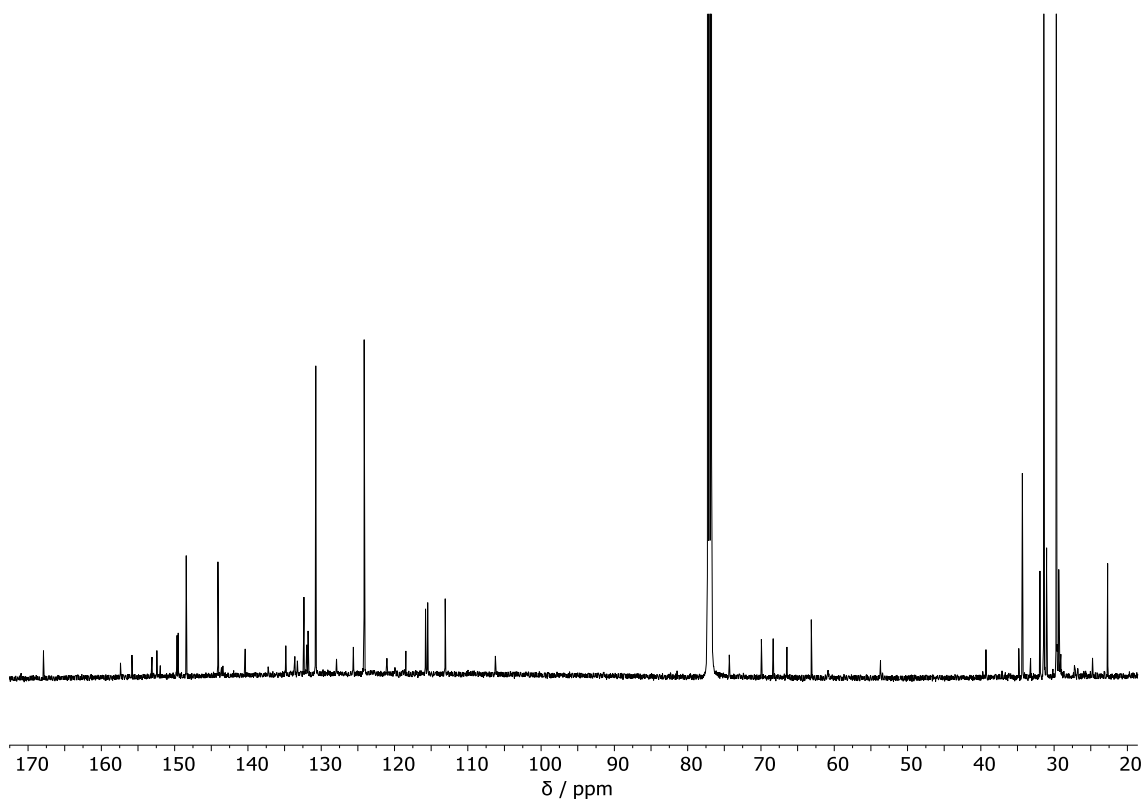


Figure S2. $^{13}\text{C}\{^1\text{H}\}$ NMR spectrum (126 MHz, CDCl_3 , 298 K) of **4·Zn**.

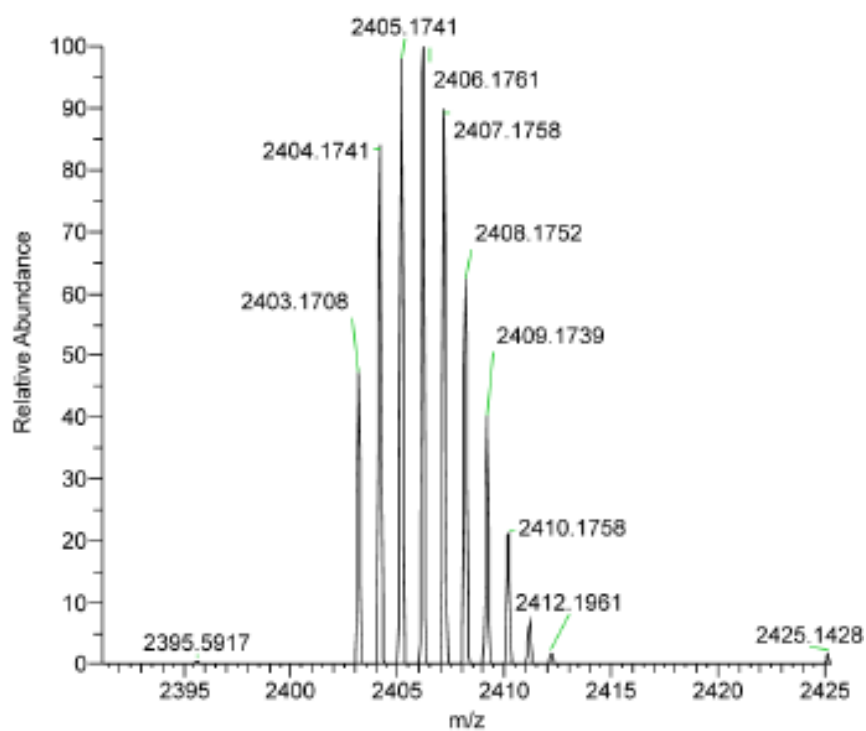


Figure S3. Measured High-Resolution ESI-MS of $4 \cdot \text{Zn}$.

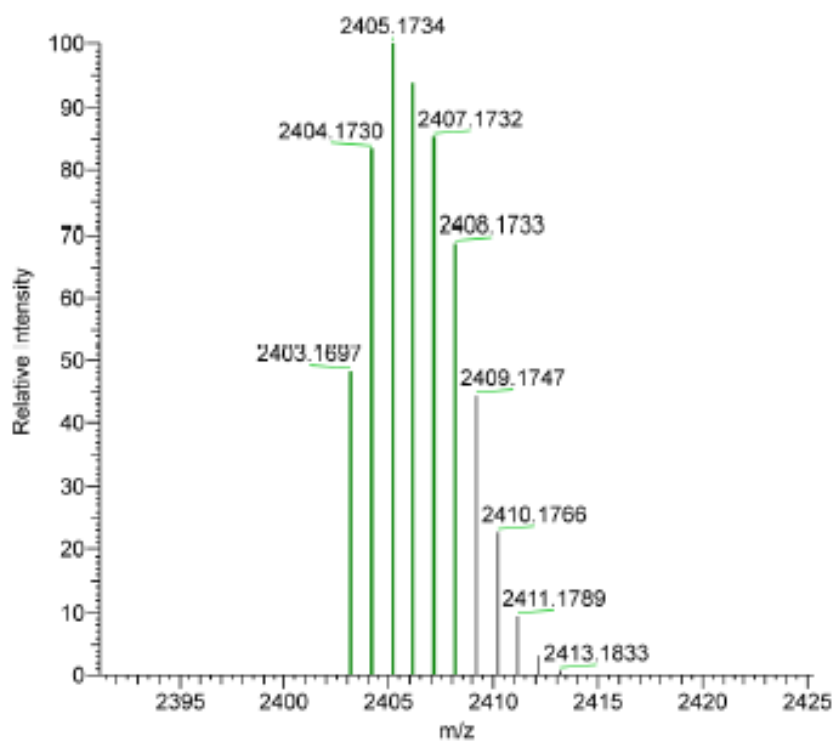


Figure S4. Theoretical High-Resolution ESI-MS of $[\text{C}_{153}\text{H}_{160}\text{O}_{10}\text{N}_{13}\text{Zn}]^+$, $[4 \cdot \text{Zn} + \text{H}]^+$.

4·H₂

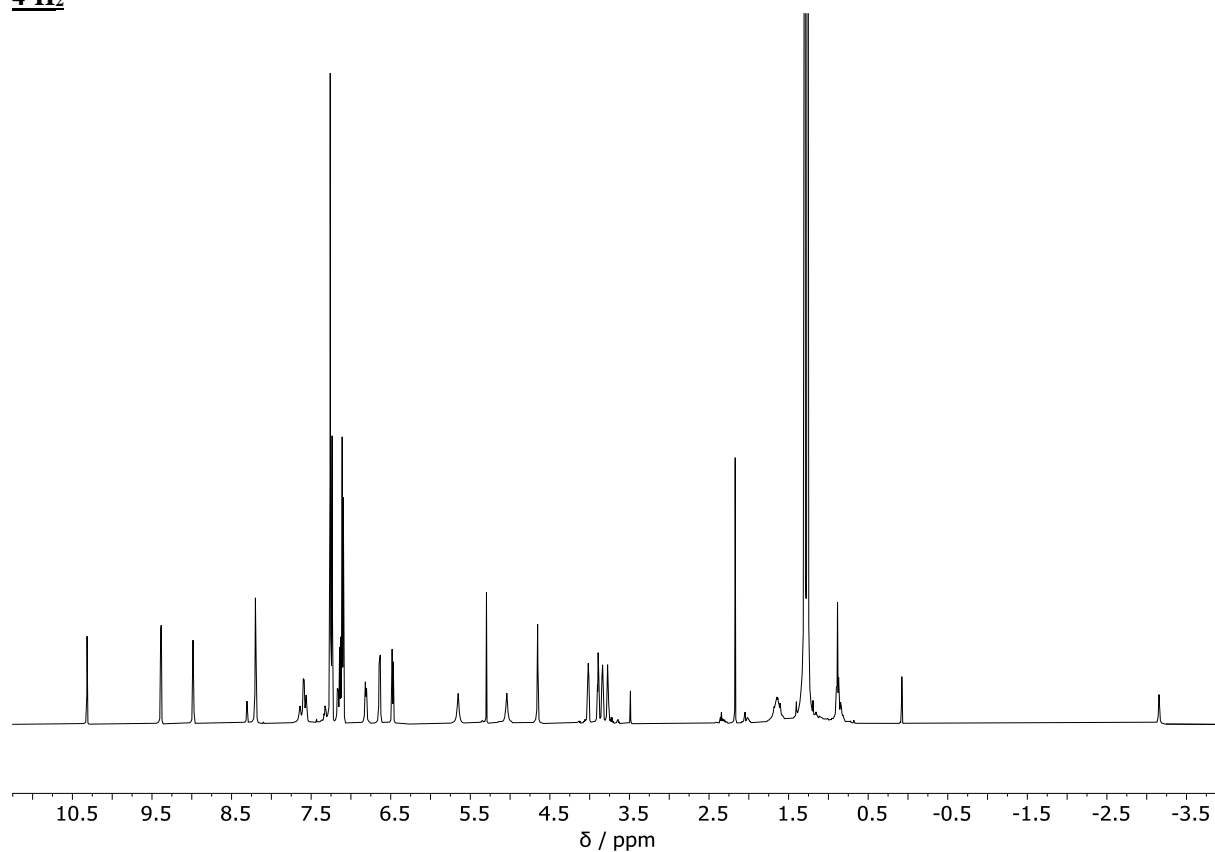


Figure S5. ¹H NMR spectrum (600 MHz, CDCl₃, 298 K) of **4·H₂**.

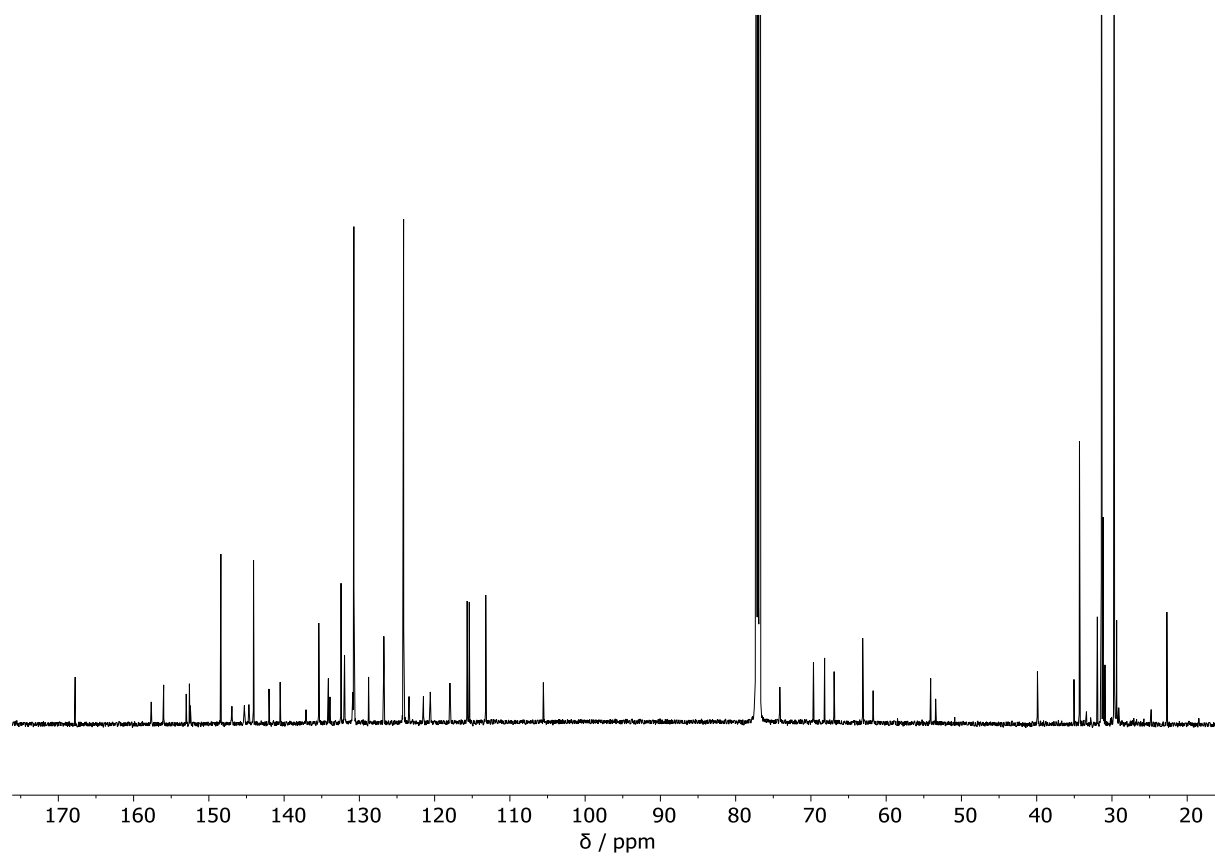


Figure S6. ¹³C{¹H} NMR spectrum (126 MHz, CDCl₃, 298 K) of **4·H₂**.

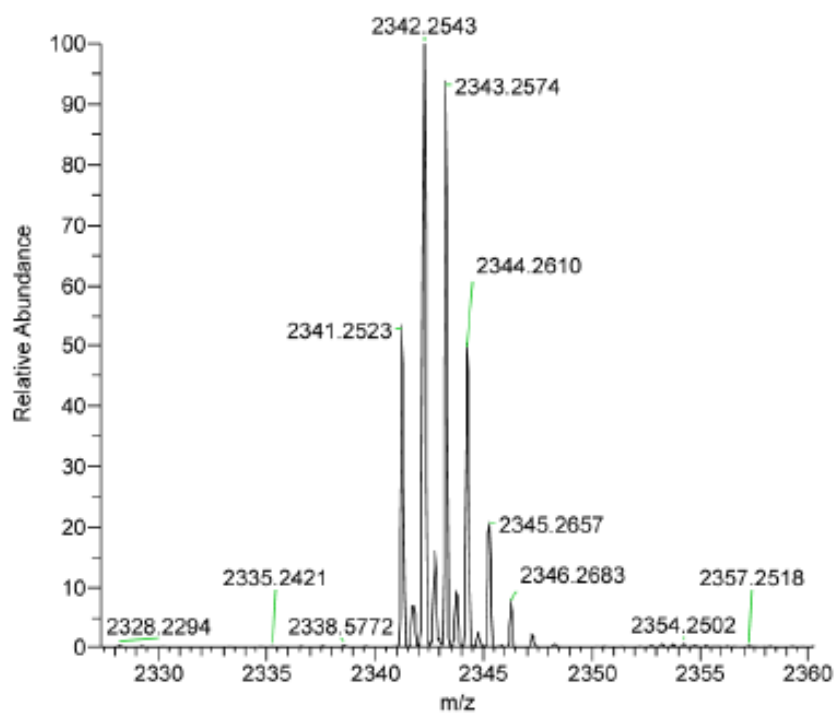


Figure S7. Measured High-Resolution ESI-MS of $4 \cdot H_2$.

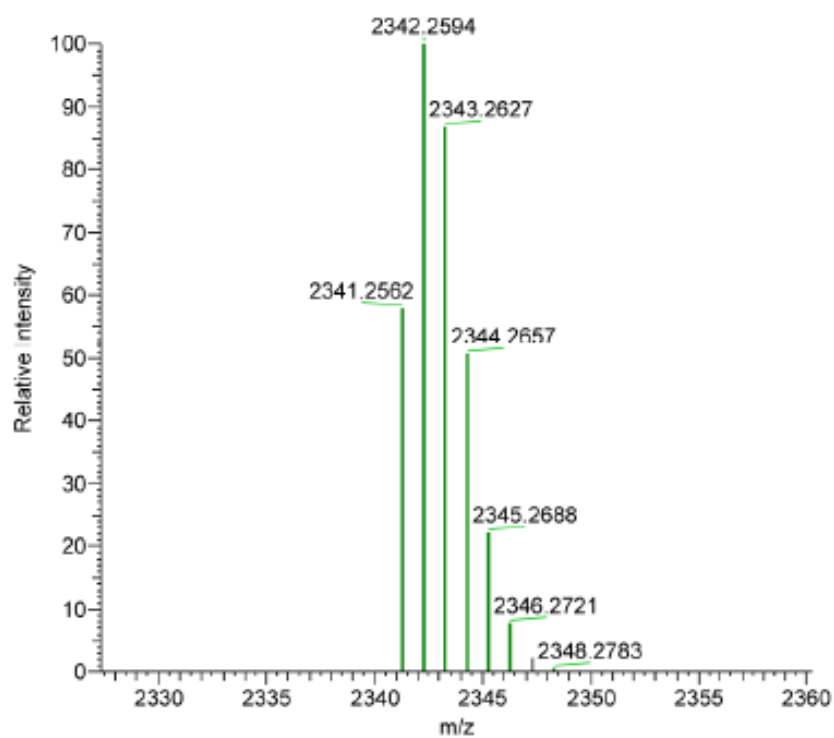


Figure S8. Theoretical High-Resolution ESI-MS of $[C_{153}H_{162}O_{10}N_{13}]^+$, $[4 \cdot H_2 + H]^+$.

S4 Investigation of Macrocycle Shuttling Barrier

Variable temperature ^1H NMR spectroscopic experiments were conducted on a 1 mM CDCl_3 solution of the $4\cdot\text{Zn}$ at 500 MHz from 233 K to 333 K. The rate constants were calculated from the spectral linewidths (in the fast-exchange regime) and peak splitting (slow-exchange regime) for porphyrin proton H_2 and thermodynamic activation parameters calculated from Eyring plots (Figure S9).⁵ A representative example of the changes in the NMR spectra, those observed on heating $4\cdot\text{Zn}$, is depicted in Figure S10.

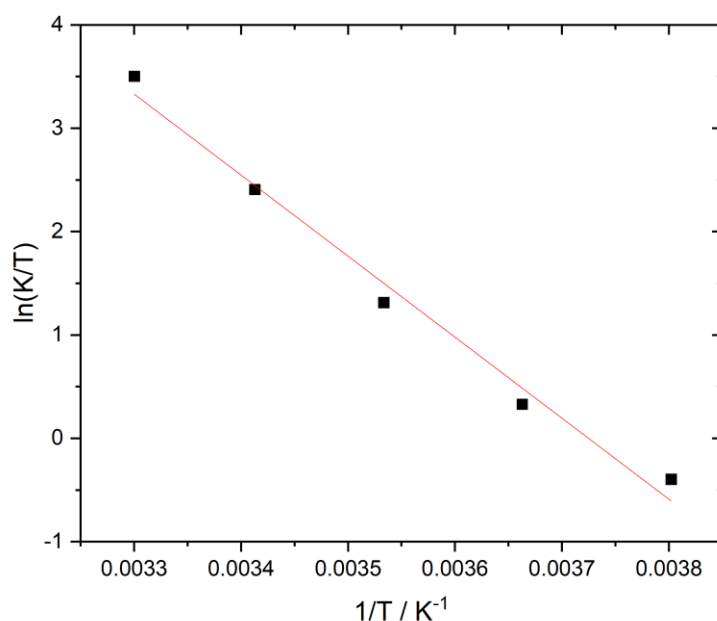


Figure S9. Eyring plots for $4\cdot\text{Zn}$ determined by ^1H VT-NMR spectroscopy (1mM in CDCl_3).

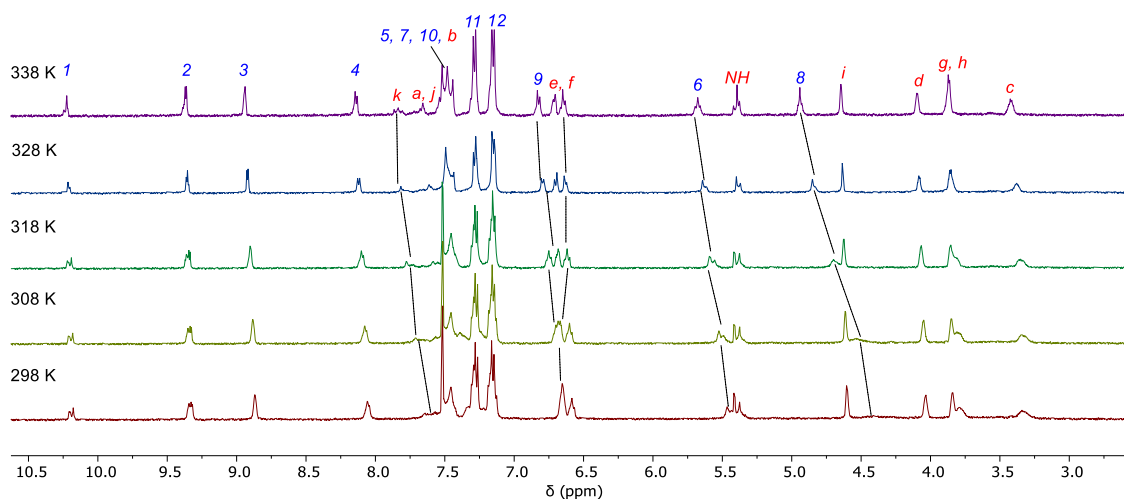


Figure S10. Stacked ^1H NMR spectra (500 MHz, CDCl_3) of $4\cdot\text{Zn}$ at indicated temperatures.

S5 Measurement of the ‘Resting State’ Bias

As the variable temperature NMR studies revealed a significant barrier to macrocycle translocation, and the increased resolution of the room temperature ^1H NMR spectrum of **4·H₂** compared to that of **4·Zn** demonstrating this interaction arose as a result of Lewis acid–base interactions between the macrocycle and axle metalloporphyrin, studies were undertaken to quantify the bias of the resting state introduced by this interaction. Given the documented significantly higher binding affinity for alkyl-substituted pyridines to Zn(II) tetraphenyl porphyrin than ether oxygen donors,^{6, 7} we assigned this interaction to a favourable pyridyl···Zn(II) interaction. Such an assignment is consistent with previous reports of Zn(II) metalloporphyrin-containing interlocked structures.^{8,9}

In order to quantify the bias for the resting state, the binding constant of **4·Zn** and pyridine, K_{rot} , was calculated. Assuming that free pyridine and the macrocycle bind to the Zn(II) centre with the same binding mode, this binding constant and the binding constant of **5·Zn** and pyridine, K_{ax} , can be used to calculate the equilibrium constant for the resting state, K_{rs} , using equation 1.⁹

$$K_{\text{rs}} = \frac{K_{\text{ax}}}{K_{\text{rot}}} - 1 \text{ (eq. 1)}$$

UV-visible titration anion binding experiments were performed at 298 K using a Horiba Duetta Fluorescence and Absorbance Spectrometer. **4·Zn** was dissolved in CHCl_3 at a concentration of 7.5 μM and its UV-visible spectra measured upon successive addition of 25 mM pyridine solution. The change in Soret band intensity was fitted to a 1:1 host:guest binding stoichiometry using a global fit of all data points in the range 412–423 nm.¹⁰

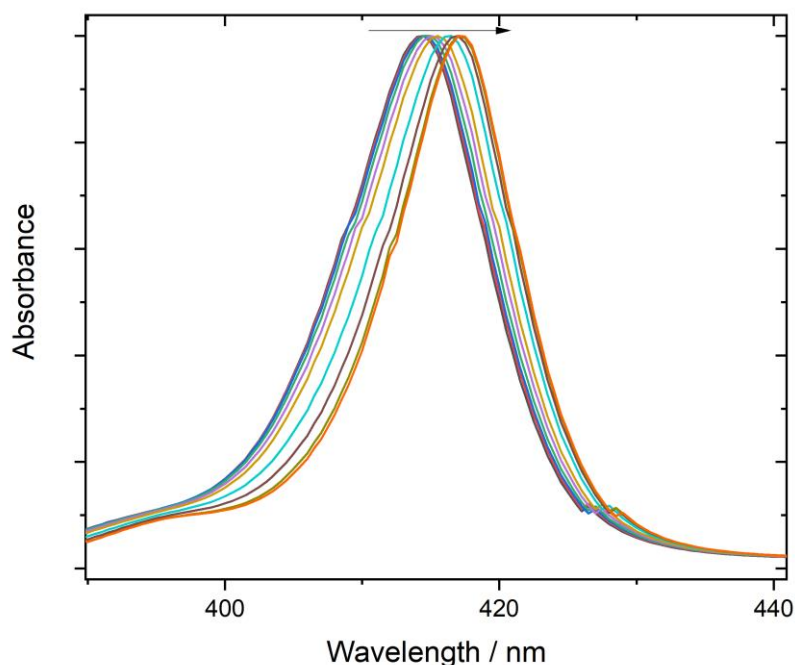


Figure S11. UV-Visible spectra of Soret band of 7.5 μM **4·Zn** solutions in CHCl_3 , upon successive addition of 25 mM pyridine. Black arrow indicates bathochromic direction of shift.

S6 ^1H NMR Binding Studies

^1H NMR titrations were recorded on a Bruker Avance III NMR spectrometer equipped with a 11.75 T magnet at 298 K. Unless stated otherwise, titrations were carried out by successive addition of a 50 mM stock solution of the target guest to a 1 mM solution of host, such that 1.0 equivalent of guest corresponds to a 10.0 μL stock solution addition. The sample was thoroughly mixed by inversion of the NMR tube prior to each spectrum being collected. 17 data points were collected, upon addition of 0.0, 0.2, 0.4, 0.6, 0.8, 1.0, 1.2, 1.4, 1.6, 1.8, 2.0, 2.5, 3.0, 4.0, 5.0, 7.5 and 10.0 equivalents of guest. All systems for which binding constants are quoted displayed fast NMR exchange at 298 K. Representative ^1H NMR titration stacks for are displayed below for titration of **4·Zn** and TBABr in the absence and presence of 1 equivalent of LiClO_4 .

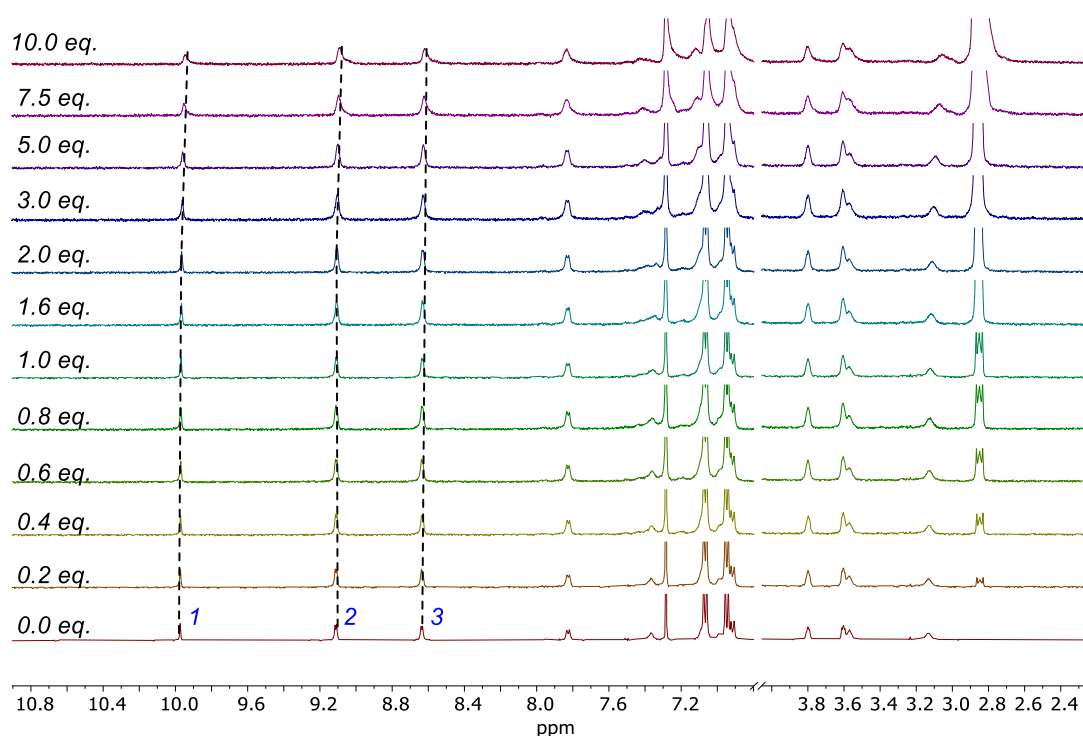


Figure S12. Stacked truncated ^1H NMR (500 MHz, 7:3 v/v $\text{CDCl}_3:\text{CD}_3\text{CN}$, 298 K) spectra of **4·Zn** upon successive additions of TBABr.

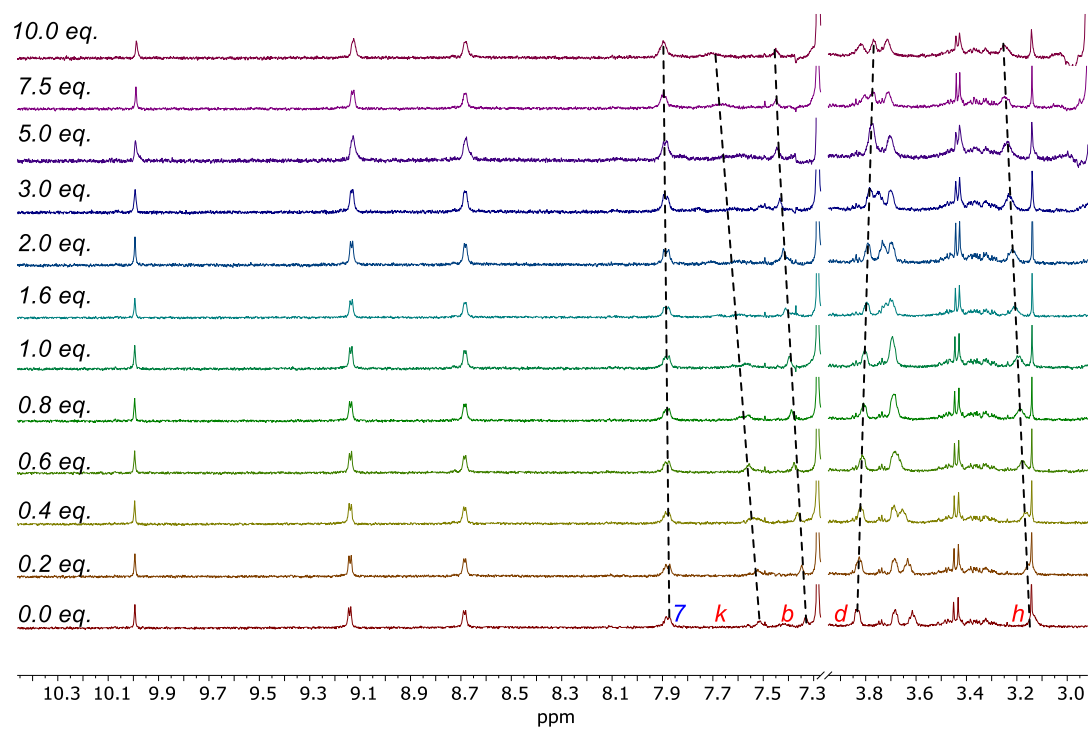
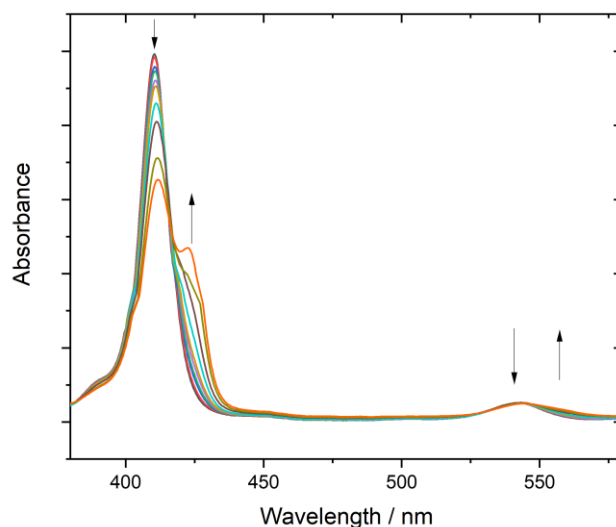


Figure S13. Stacked truncated ^1H NMR (500 MHz, 7:3 v/v CDCl_3 : CD_3CN , 298 K) spectra of an equimolar solution of **4-Zn** and LiClO_4 upon successive additions of TBABr.

S7 Optical Titration Studies of TBAX Salt Anion Binding

UV-visible titration anion binding experiments were performed at 298 K using a Horiba Duetta. The receptor was dissolved in acetone at a concentration of 2 μM . Unless otherwise stated, the TBA salt of the anionic guest was dissolved in the stock solution at a concentration of 100 mM. Aliquots of the guest solution were added to 1.0 mL of the host solution in a quartz glass cuvette. The sample was then mixed and the UV-visible spectra recorded upon successive additions of the TBA salt solution. The absorbance intensities at 411 nm (maximum of free host Soret band absorption), and 422 nm (maximum of host-guest complex Soret band absorption) were plotted, and the resulting isotherms globally fitted to a 1:1 stoichiometric host-guest binding model.¹⁰

a)



b)

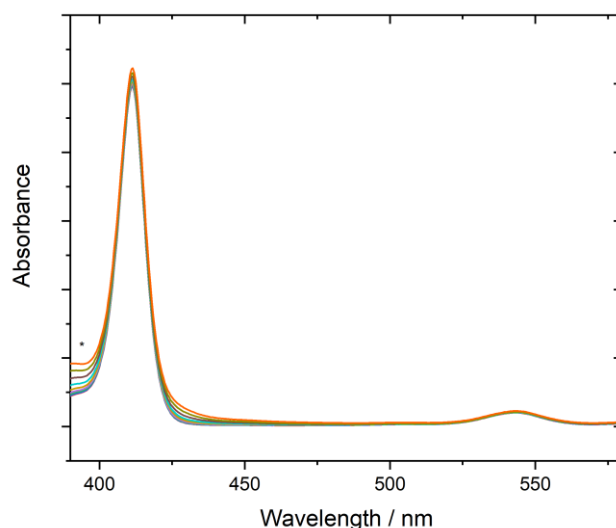
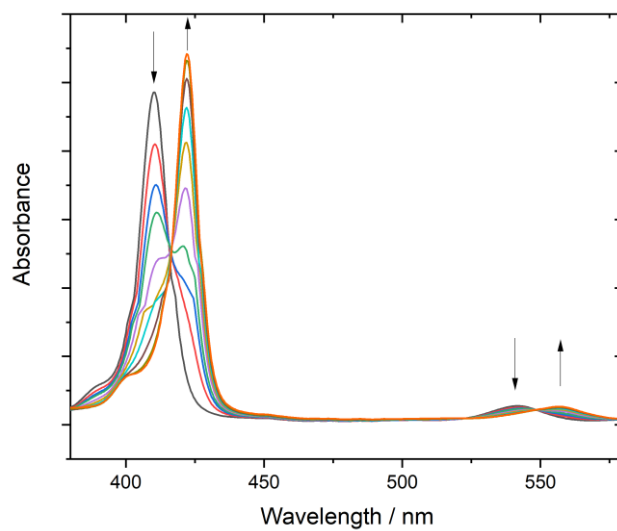


Figure S14. UV-Visible spectra of Soret and Q-bands of 2 μM **4·Zn** solutions in acetone, upon successive addition of 100 mM TBAX salts. a) X = Br, b) X = I. Black arrows indicate direction of change. * Rise in low wavelength intensity of TBAI solution attributed to formation of trace amounts of triiodide (I_3^-) species in TBAI solution.

a)



b)

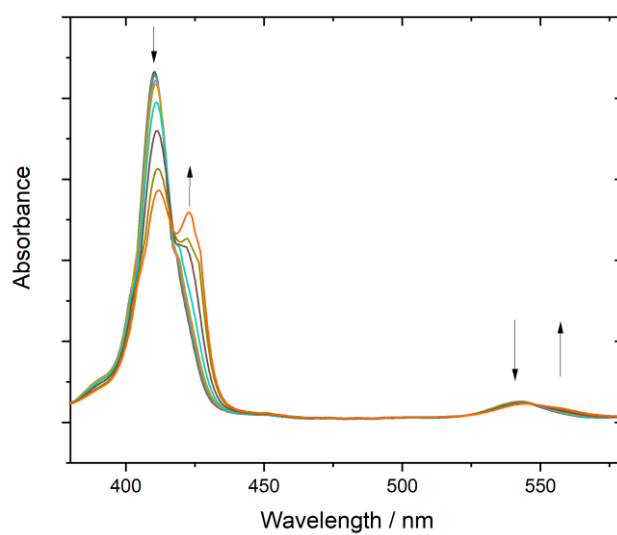


Figure S15. UV-Visible spectra of Soret and Q-bands of $2 \mu\text{M } 4\text{-Zn}\cdot\text{Li}^+\text{X}^-$ solutions in acetone, upon successive addition of 100 mM TBAX salts. a) X = Cl, b) X = Br. Black arrows indicate direction of change.

S8 References

1. A. Brown, T. Lang, K. M. Mullen and P. D. Beer, *Org. Biomol. Chem.*, 2017, **15**, 4587-4594.
2. D. A. Roberts, T. W. Schmidt, M. J. Crossley and S. Perrier, *Chem. Eur. J.*, 2013, **19**, 12759-12770.
3. A. Tron, P. J. Thornton, M. Rocher, H.-P. Jacquot de Rouville, J.-P. Desvergne, B. Kauffmann, T. Buffeteau, D. Cavagnat, J. H. R. Tucker and N. D. McClenaghan, *Org. Lett.*, 2014, **16**, 1358-1361.
4. V. Aucagne, K. D. Hänni, D. A. Leigh, P. J. Lusby and D. B. Walker, *J. Am. Chem. Soc.*, 2006, **128**, 2186-2187.
5. H. Eyring, *J. Chem. Phys.*, 1935, **3**, 107-115.
6. C. H. Kirksey, P. Hambright and C. B. Storm, *Inorg. Chem.*, 1969, **8**, 2141-2144.
7. J. V. Nardo and J. H. Dawson, *Inorg. Chim. Acta*, 1986, **123**, 9-13.
8. J. T. Wilmore, Y. Cheong Tse, A. Docker, C. Whitehead, C. K. Williams and P. D. Beer, *Chem. Eur. J.*, 2023, **29**, e202300608.
9. S. W. Hewson and K. M. Mullen, *Org. Biomol. Chem.*, 2018, **16**, 8569-8578.
10. D. Brynn Hibbert and P. Thordarson, *Chem. Commun.*, 2016, **52**, 12792-12805.